



# Conspicuity and muscle-invasiveness assessment for bladder cancer using VI-RADS: a multi-reader, contrast-free MRI study to determine optimal b-values for diffusion-weighted imaging

Andrea Delli Pizzi<sup>1</sup> · Domenico Mastrodicasa<sup>2</sup> · Alessio Taraschi<sup>3</sup> · Nicoletta Civitareale<sup>3</sup> · Erica Mincuzzi<sup>3</sup> · Stefano Censi<sup>4</sup> · Michele Marchioni<sup>5,6</sup> · Giulia Primiceri<sup>5</sup> · Pietro Castellan<sup>5</sup> · Roberto Castellucci<sup>5</sup> · Giulio Cocco<sup>7</sup> · Piero Chiacchiaretta<sup>8,9</sup> · Antonella Colasante<sup>10</sup> · Antonio Corvino<sup>11</sup> · Luigi Schips<sup>5</sup> · Massimo Caulo<sup>4</sup>

Received: 2 February 2022 / Revised: 7 March 2022 / Accepted: 7 March 2022 / Published online: 18 March 2022  
© The Author(s) 2022

## Abstract

**Objective** To (1) compare bladder cancer (BC) muscle invasiveness among three b-values using a contrast-free approach based on Vesical Imaging-Reporting and Data System (VI-RADS), to (2) determine if muscle-invasiveness assessment is affected by the reader experience, and to (3) compare BC conspicuity among three b-values, qualitatively and quantitatively.

**Methods** Thirty-eight patients who underwent a bladder MRI on a 3.0-T scanner were enrolled. The gold standard was histopathology report following transurethral resection of BC. Three sets of images, including T2w and different b-values for DWI, set 1 ( $b = 1000 \text{ s/mm}^2$ ), set 2 ( $b = 1500 \text{ s/mm}^2$ ), and set 3 ( $b = 2000 \text{ s/mm}^2$ ), were reviewed by three differently experienced readers. Descriptive statistics and Intraclass Correlation Coefficient (ICC) were calculated. Comparisons among readers and DWI sets were performed with the Wilcoxon test. Receiver operating characteristic (ROC) analysis was performed. Areas under the curves (AUCs) and pairwise comparison were calculated.

**Results** AUCs of muscle-invasiveness assessment ranged from 0.896 to 0.984 (reader 1), 0.952–0.968 (reader 2), and 0.952–0.984 (reader 3) without significant differences among different sets and readers ( $p > 0.05$ ). The mean conspicuity qualitative scores were higher in Set 1 (2.21–2.33), followed by Set 2 (2–2.16) and Set 3 (1.82–2.14). The quantitative conspicuity assessment showed that mean normalized intensity of tumor was significantly higher in Set 2 (4.217–4.737) than in Set 1 (3.923–4.492) and Set 3 (3.833–3.992) ( $p < 0.05$ ).

**Conclusion** Muscle invasiveness can be assessed with high accuracy using a contrast-free protocol with T2W and DWI, regardless of reader's experience.  $b = 1500 \text{ s/mm}^2$  showed the best tumor delineation, while  $b = 1000 \text{ s/mm}^2$  allowed for better tumor–wall interface assessment.

**Keywords** Bladder cancer · VI-RADS · MRI · Diffusion-weighted imaging

## Abbreviations

ADC	Apparent diffusion coefficient
BC	Bladder cancer
MRI	Magnetic resonance imaging
DCE	Dynamic contrast enhanced
DWI	Diffusion-weighted imaging
MIBC	Muscle-invasive bladder cancer
NMIBC	Non-muscle-invasive BC
T2W	T2W-weighted images

TURB	Transurethral resection of the bladder
VI-RADS	Vesical imaging-reporting and data system

## Introduction

Bladder cancer (BC) is a leading cause of cancer-related death in men and accounts for approximately 550,000 new cancer cases per year worldwide [1]. Muscle-invasive BC (MIBC) represents about a quarter of the total and is > T1 tumor (growth into the muscle layer). MIBC usually requires radical cystectomy, with or without neo- or adjuvant chemotherapy, thus significantly impacting patients' survival [2]. Non-muscle-invasive BC (NMIBC) (Ta–T1 tumor) may usually benefit from local treatments and has a better prognosis

✉ Andrea Delli Pizzi  
andreadellipizzi@gmail.com

Extended author information available on the last page of the article

[3]. Accurate preoperative staging of bladder cancer is essential in determining the extent of disease and optimal treatment. Magnetic resonance imaging has recently gained traction due to its accuracy for the local staging and the assessment of muscle invasiveness [4–9]. This is largely due to the combination of high-resolution anatomical sequence (T2-weighted images—T2W) with functional sequences (Diffusion-Weighted Imaging—DWI, and Dynamic Contrast Enhanced—DCE), especially when using high field strength (3.0-T) [4, 10, 11]. In 2018, Vesical Imaging-Reporting And Data System (VI-RADS) introduced a standardized reporting criterion for bladder MRI to improve communication among doctors and facilitate patient management [5]. Several studies demonstrated high accuracy of VI-RADS for discriminating MIBC and NMIBC [12–16]. The standard MR protocol is currently defined “three-parametric” and includes conventional T2W images, DWI, and DCE imaging. Among these sequences, DWI has been considered the most relevant sequence to estimate muscle invasion [5]. A study investigating the feasibility of contrast-free MR imaging was recently proposed [17]. The authors reported that the diagnostic accuracy of a contrast-free MR imaging protocol, including only T2w and DWI, was comparable to the standard three-parametric protocol for the detection of MIBC, regardless of the reader experience. However, to the best of our knowledge, the best diffusion gradient strengths (*b*-values) to evaluate muscle invasiveness and tumor conspicuity have yet to be defined. Based on recent studies assessing different tumor type conspicuity using different diffusion gradient strengths, two are the most relevant issues [18–25]. On the one hand, a high diffusion gradient strength would provide a better background suppression, thus allowing an easier delineation of the tumor. On the other hand, it may result in a reduced signal-to-noise ratio with a subsequent overall decreased signal intensity and anatomical detail [26]. This approach may have a twofold beneficial effect. First, considering the emerging role of VI-RADS, it may help to optimize the standard MR imaging protocol. Second, in a contrast-free MR imaging setting, it may have a beneficial impact on costs, scan time, and patient safety, especially considering the potential future extension of VI-RADS to the surveillance and treatment response assessment [27, 28]. For these reasons, in this proof-of-concept study, we aimed to (1) compare the muscle invasiveness of tumor among three different *b*-values using a VI-RADS-based contrast-free approach, to (2) determine if the muscle-invasiveness assessment is affected by the reader experience, and to (3) compare the conspicuity of bladder cancer among three different *b*-values both qualitatively and quantitatively.

## Material and methods

### Patient population and study design

An Institutional Review Board and Ethical Committee approval were received for this prospective study. The study was performed in line with the European Urology and Good Clinical Practice guidelines and conducted accordingly to ethical principles laid down by the latest version of the Declaration of Helsinki [7]. Written informed consent was obtained from all patients enrolled in the study. A total of 41 patients who underwent multiparametric-MRI (mp-MRI) between August 2019 and December 2019 were prospectively included. The study population was previously described in detail [16, 17]. For this study the inclusion criteria were 1) endoscopic findings suggestive of BC, 2) MRI of bladder performed on a 3-T scanner, and 3) TURB with histological evaluation. Finally, three patients were excluded: two patients for severe artifacts in the pelvis (one patient showed susceptibility artifacts due to hip replacement and one patient showed motion artifacts on DWI) and one patient was scanned on a 1.5 T scanner. The final study population was composed of 38 patients.

### MRI protocol

A state-of-the-art 3-T MR scanner (dStream, Philips Medical System, Best, the Netherlands) equipped with a phased array surface coil was used for all patients included in the study. The MR protocol included the following sequences: T2W turbo spin-echo images, DWI (including  $b=1000$  s/mm<sup>2</sup>,  $b = 1500$  s/mm<sup>2</sup>,  $b = 2000$  s/mm<sup>2</sup>) and DCE T1-weighted 3D spoiled gradient-echo images (DCE). A more detailed description of the MR parameters is reported in Table 1. Apparent diffusion coefficient maps (ADC maps) were calculated for each patient. Gadoteridol (Prohance; Bracco, Milan, Italy) was used in a dose of 0.2 mmol/kg (flow rate of 2 mL/s). Patients received 20 mg of scopolamine butylbromide (Buscopan, Boehringer Ingelheim, Ingelheim am Rhein, Germany) intravenously to reduce the incidence of motion artifacts due to bowel motility. Patients were instructed to void 1–2 h before imaging and started drinking 500–1000 ml of water 30 min before the examination [5]. The degree of bladder filling was evaluated using ultrasound before patient entered the MR room.

### Image analysis

Three sets of images, namely set 1, set 2, and set 3, were evaluated on a dedicated workstation. Each set included axial, sagittal, and coronal T2W images and DWI images

**Table 1** Parameters of T2-weighted and DWI sequences included in the three sets of images

	Set 1	Set 2	Set 3	Set 1	Set 2	Set 3
	T2cb-weighted Fast-Spin Echo			Diffusion-Weighted Imaging (DWI)*		
Repetition time (ms)	3000–5000			3000		
Echo time (ms)	80			97		
Matrix	200 × 179			68 × 54		
Flip angle	90			90		
Number of excitations	2			3–12		
Section thickness (mm)	4			4		
<i>b</i> -value ( s/mm <sup>2</sup> )	–			1000	1500	2000
Imaging planes	Transverse <sup>†</sup> , Coronal, Sagittal			Transverse <sup>†</sup> , Sagittal		
Acquisition time (min)	2.26			4.19		

DWI sequences included ADC map calculation

\*DWI performed with *b*-values of 0, 600, 1000, 1500, and 2000 s/mm

<sup>†</sup>Transverse plane angulated perpendicularly to the long axis of the bladder

**Table 2** Descriptive baseline characteristics of included patients (*n* = 38)

Features	Value
Age	72.5 (66.5–81.0)
Gender, Male	27 (71.4%)
Body mass index, kg/m <sup>2</sup>	26.6 (24.0–29.1)
<i>Charlson Comorbidity Index</i>	
0	21 (55.3%)
1	13 (34.2%)
2	3 (7.9%)
3	1 (2.6%)
<i>Urine cytology</i>	
Non-diagnostic	13 (34.2%)
Negative	16 (42.1%)
Positive	9 (23.7%)
<i>Previous endovascular treatment</i>	
Bacillus Calmette-Guerin	4 (10.5%)
Epirubicin	1 (2.6%)
Mitomycin C	3 (7.9%)
None	30 (78.9%)

Continuous variables are presented as median and interquartile ranges (IQR). Categorical variables are presented as frequencies and percentages (%)

with the corresponding ADC map. In detail, *b* = 1000 s/mm<sup>2</sup> images were included in set 1, *b* = 1500 s/mm<sup>2</sup> images in Set 2, and *b* = 2000 s/mm<sup>2</sup> in set 3. Each set of images included axial and sagittal planes and was randomly assigned to three readers with different levels of experience in abdominal radiology (1 radiologist with 10 years of expertise in abdominal MRI, one senior resident with two years of expertise in abdominal MRI, and one second-year resident with 1 year of expertise in

abdominal MRI) in three separate reading sessions with at least a month in between, to avoid recall bias (Table 2).

### Muscle-invasiveness assessment

MRI criteria for muscle invasiveness were assessed according to VI-RADS as well as the bladder subdivision in sectors [5, 16]. In this way, twelve sectors were considered. Following VI-RADS, all detected lesions were scored on a 5-point scale based on the likelihood of muscle invasion: 1, highly unlikely; 2, unlikely; 3, equivocal; 4, likely; and 5, very likely [5].

### Qualitative conspicuity assessment

The three readers independently qualitatively assessed 3 sets of images. In detail, they scored the tumor conspicuity on DWI using a 3-point scale: (1) hyperintense lesion, but only slightly demarcated from the background and/or poor tumor–wall interface, (2) hyperintense lesion, well demarcated from the background with good tumor–wall interface, and (3) hyperintense lesion with excellent background suppression and optimal tumor–wall interface (Fig. 1). The T2w images were available to the readers for anatomical reference.

### Quantitative conspicuity assessment

To quantitatively assess the tumor conspicuity, the expert reader used a circular 5-mm<sup>2</sup> region of interest (ROI) of the tumor on DWI images using T2-weighted images for anatomical reference (Fig. 2). In detail, a single-slice measurement was performed by placing three ROIs randomly in the tumor and calculating the mean tumor intensity. A circular 5-mm<sup>2</sup> region of interest was also placed in the bladder content to normalize

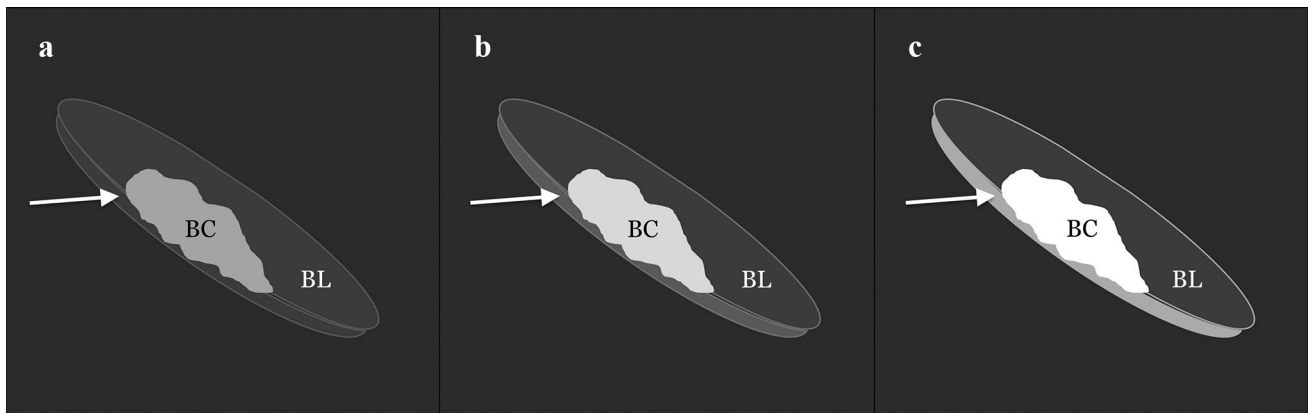


**Fig. 1** Three-point scale used to assess tumor conspicuity on DWI: **a** hyperintense lesion, but only slightly demarcated from the background and/or poor tumor–wall interface, **b** hyperintense lesion, well demarcated from the background with good tumor–wall interface,

and **c** hyperintense lesion with excellent background suppression and optimal tumor–wall interface. BC = bladder cancer; arrow = bladder wall; BL = bladder lumen

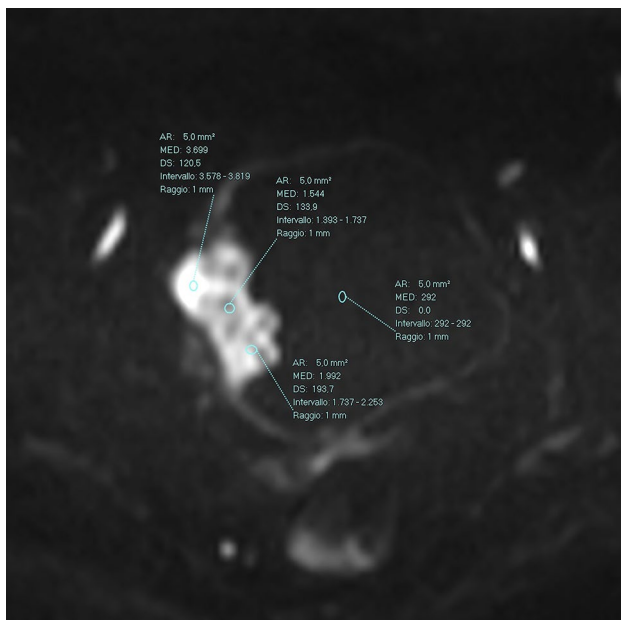


**Fig. 2** Quantitative analysis. Three circular 5-mm<sup>2</sup> regions of interest (ROIs) of the tumor were placed on DWI images. Another circular 5-mm<sup>2</sup> ROI was also placed in the bladder content to normalize data. Tumor conspicuity was defined as the ratio between the mean tumor intensity and the bladder content intensity

data. Tumor conspicuity was defined as the ratio between the mean tumor intensity and the bladder content intensity.

## Reference standard

Urologic evaluation included the description of lesion number, size, morphology, and location. A standardized form with a descriptive schematic map was used for cystoscopy, MRI, and TURB, to record all the information on each lesion [16]. All patients underwent a standard TURB and a piecemeal resection in fraction. The base of each lesion was sent to histological evaluation separately with a numerical code to compare histological results with those of cystoscopy and mp-MRI. When indicated, a second TURB was performed according to the EAU guidelines [7]. Specimens were examined to assess the type, grade, and stage of the tumor. The World Health Organization classification was used to classify and grade malignant tumors, while the American Joint Committee on Cancer/Union for International Cancer Control TNM system was used to stage each lesion [7].

## Statistical analysis

Sample size estimation was performed considering the association between VI-RADS score and MIBC status. The reference was the proportion of NMIBC and MIBC stratified according to VI-RADS score in previous studies [16, 29]. A power of 90% and a value of 5% were considered for the  $\chi^2$  test. Sample size was estimated using the R package “pwr” (version 1.2.2; function: pwr.chisq.test). The estimated effect size was 0.7, and the number of patients needed to obtain the desired power was 31 subjects. A dichotomization of VI-RADS scores was performed. In detail, concerning the diagnostic accuracy for the detection of MIBC, VI-RADS scores of 1–3 were considered negative, while VI-RADS scores of 4–5 were considered positive. Descriptive statistics

and Intraclass Correlation Coefficient (ICC) were calculated for each reader. Comparison among readers and sets was achieved with Wilcoxon test. Receiver operating characteristic (ROC) analysis was performed, and areas under the curve (AUCs) were calculated for each reader and image set. ROC curves were compared to test the difference between the areas under the ROC curves among the three readers. ROC curve comparison was performed with MedCalc software, version 16.8.4 (MedCalc Software, Ostend, Belgium). All other statistical analyses were performed using IBM SPSS Statistics software, version 20 (IBM, Armonk, NY). A  $p$ -value  $\leq 0.05$  was considered statistically significant.

## Results

Twenty-seven patients of the study were male (27, 71%) with a median age of 72.5 (IQR 66.5–81.0) years. Out of the 38 patients, 31 (82%) had a NMBIC (Ta–T1) and 7 (18%) had a MIBC (T2–T3). Sixty-eight BCs were diagnosed of which 33 (48.5%) were Ta (non-invasive papillary carcinoma), 28 (41.2%) were T1 (subepithelial connective tissue invasion),

6 (8.8%) were T2 (muscle invasion), and 1 (1.5%) was T3 (perivesical tissue invasion) [30]. The mean dimension, measured at cystoscopy, of NMIBC was 9.8 mm (range 3–40 mm), while the mean dimension of MIBC was 29 mm (range 10–50 mm).

## Muscle-invasiveness assessment

The 7 MIBCs were correctly identified by all readers using every set of images. Table 3 shows the diagnostic performance of the readers for the MIBC detection. In detail, no significant differences were observed in diagnostic performance for all readers among the 3 sets of images ( $p > 0.05$ ). The AUCs for the three sets of images ranged from 0.896 to 0.984 (reader 1), 0.952 to 0.968 (reader 2), and 0.952 to 0.984 (reader 3), respectively. No significant differences in diagnostic performance were found among the three readers in the pairwise comparison ( $p > 0.05$ ). Table 4 shows a per-lesion diagnostic performance analysis for each reader to classify BCs according to the TNM classification. False-positive cases occurred only in

**Table 3** Diagnostic performance of the three readers regarding the MIBC detection for Set 1, Set 2, and Set 3

	AUC MIBC vs. NMIBC (Standard error)			Pairwise readers	$p$ -value
	Set 1	Set 2	Set 3		
<i>Reader 1</i>	0.896 (0.075)	0.968 (0.022)	0.984 (0.016)	Reader 1 vs Reader 2	> 0.05
<i>Reader 2</i>	0.968 (0.022)	0.952 (0.027)	0.968 (0.022)	Reader 1 vs Reader 3	> 0.05
<i>Reader 3</i>	0.952 (0.027)	0.952 (0.027)	0.984 (0.016)	Reader 3 vs Reader 2	> 0.05

**Table 4** Per-lesion diagnostic performance of the three readers to correctly classify BCs according to TNM Stage Classification

		Set 1			Set 2			Set 3		
		Correctly Classified	Incorrectly Classified		Correctly Classified	Incorrectly Classified		Correctly Classified	Incorrectly Classified	
			False Negatives	False Positives		False Negatives	False Positives		False Negatives	False Positives
Ta ( $n=33$ )	<i>Reader 1</i>	22	11	0	20	11	2	19	14	0
	<i>Reader 2</i>	25	8	0	24	8	1	23	10	0
	<i>Reader 3</i>	20	11	2	20	11	2	20	12	1
T1 ( $n=28$ )	<i>Reader 1</i>	24	2	2	26	1	1	24	3	1
	<i>Reader 2</i>	24	2	2	24	2	2	24	2	2
	<i>Reader 3</i>	25	2	1	24	2	2	25	2	1
T2 ( $n=6$ )	<i>Reader 1</i>	5	1	0	6	0	0	6	0	0
	<i>Reader 2</i>	6	0	0	6	0	0	6	0	0
	<i>Reader 3</i>	6	0	0	6	0	0	6	0	0
T3 ( $n=1$ )	<i>Reader 1</i>	1	0	0	1	0	0	1	0	0
	<i>Reader 2</i>	1	0	0	1	0	0	1	0	0
	<i>Reader 3</i>	1	0	0	1	0	0	1	0	0



NMIBCs, mostly in set 1 and set 2 (7 and 10 vs. 5 of Set 3). Out of 114 false negatives, extracted from all readers, 113 were NMIBCs. False-negative cases increased for all three readers when using Set 3 (from 12 to 17 for reader 1, from 10 to 12 the reader 2, and from 13 to 14 for reader 3). Case examples of correctly and incorrectly classified MIBC are shown in Figs. 3 and 4, respectively.

### Qualitative conspicuity

Results of the qualitative conspicuity assessment are shown in Table 5. The mean conspicuity scores were higher in Set 1 (2.21, 2.31, and 2.33 for reader 1, 2, and 3, respectively), followed by Set 2 (2, 2.16, and 2.15 for reader 1, 2, and 3, respectively) and Set 3 (2.14, 1.82, and 1.91 for reader 1, 2, and 3, respectively) for all readers. The ICC among readers was 0.75 (set 1), 0.77 (set 2), and 0.81 (set 3).

### Quantitative conspicuity

The mean normalized intensity of the tumor was significantly higher when using Set 2 (4.737, 4.217, and 4.608 for reader 1, 2, and 3, respectively) compared to Set 1 (4.123, 3.923, and 4.492 for reader 1, 2, and 3, respectively) and Set 3 (3.896, 3.992, and 3.833 for reader 1, 2, and 3, respectively). The ICC among readers was 0.79 (set 1), 0.83 (set 2), and 0.91 (set 3). Results of the quantitative conspicuity assessment and pairwise comparison are shown in Table 6.

### Discussion

Our results showed that all *b*-values included in this study accurately assessed bladder cancer muscle invasiveness using a bi-parametric MR protocol. Moreover, the reader's experience did not significantly affect the diagnostic accuracy. Our results confirmed the promising results of recent studies on the feasibility of contrast-free MRI protocols

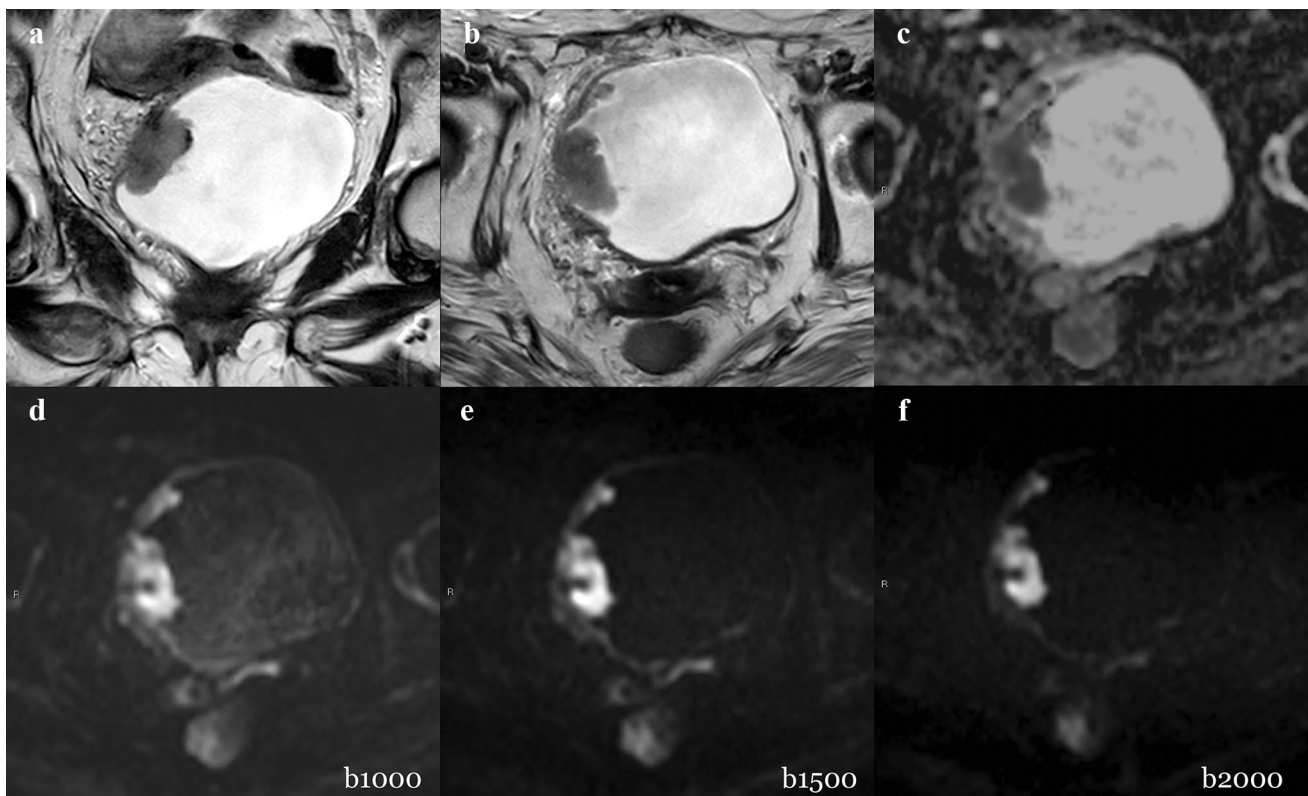


**Fig. 3** Example of muscle-invasive BC classified correctly. A 79-year-old woman with hematuria and a bladder mass reported after flexible cystoscopy underwent bladder MRI before primary TURB. Coronal (a) and axial (b) T2W imaging showed a thickened right-lateral wall. All gradient strengths (b1000, b1500, and b2000) and ADC map (c) confirmed the restricted diffusion of the tumor extending to

the muscular layer. The tumor conspicuity on b1000 (d) was higher than b1500 (e) and b2000 (f) due to better tumor–wall interface visualization. The T stage after TURB was HG-T2 (TURB). DWI = diffusion-weighted imaging; HG = high grade; MRI = magnetic resonance imaging; T2W = T2 weighted; TURB = transurethral resection of the bladder; VI-RADS = Vesical Imaging-Reporting and Data System

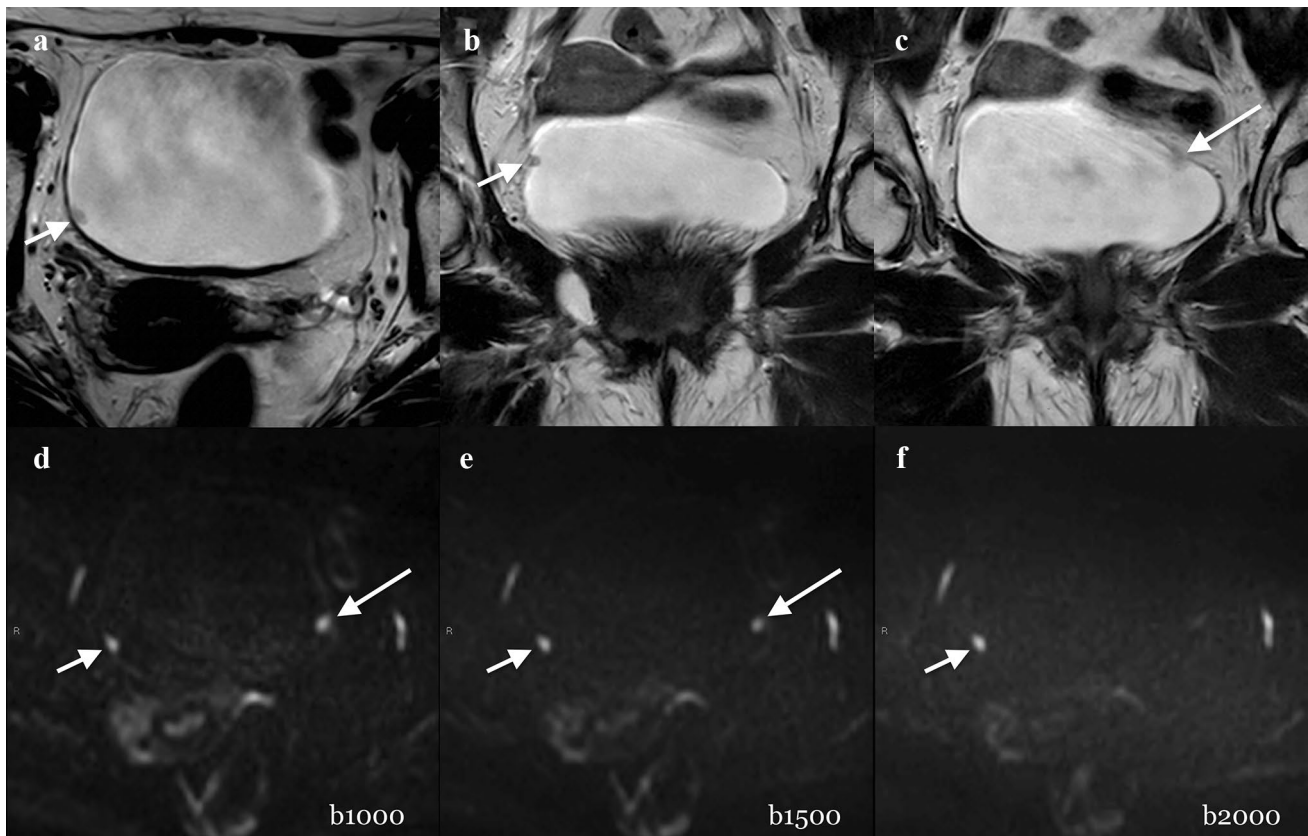


**Fig. 4** Example of a not muscle-invasive BC classified incorrectly. A 73-year-old man with hematuria and two polyps, documented after flexible cystoscopy, underwent MRI before primary TURB. Axial (a) and coronal (b, c) T2W imaging (T2) showed a small (4 mm) polypoid lesion on the right wall of the bladder (short arrow in a and b). The lesion was well detected by the three readers regardless the image set and was scored as VI-RADS 1 (short arrow in d, e, and f). Another slightly visible small (4 mm) non-muscular invasive lesion (VI-RADS 1) on the left wall of the bladder was suspected on

T2 images (long arrow in e). However, it was definitely detected by the three readers only when reading b1000 and b1500 images (long arrow in d and e), but not on b2000 images. T stage after TURB was LG-T1 (TURB). After four weeks, Re-TURB was performed and it confirmed the absence of residual tumor. DWI=diffusion-weighted imaging; HG=high grade; MRI=magnetic resonance imaging; T2W=T2 weighted; TURB=transurethral resection of the bladder; VI-RADS= Vesical Imaging-Reporting and Data System

**Table 5** Qualitative assessment of tumor conspicuity for Set 1, Set 2, and Set 3 based on a 3-point scale

	Qualitative Assessment Mean Tumor Conspicuity (Standard Deviation)			ICC (95% Confidence Intervall)		
	Set 1	Set 2	Set 3	Set 1	Set 2	Set 3
<i>Reader 1</i>	2.31 (0.69)	2.00 (0.76)	2.14 (0.87)	0.75	0.77	0.81
<i>Reader 2</i>	2.21 (0.77)	2.16 (0.75)	1.82 (0.79)	(0.60–0.85)	(0.64–0.86)	(0.70–0.89)
<i>Reader 3</i>	2.33 (0.75)	2.15 (0.78)	1.91 (0.88)			

based on DWI [5, 17, 31]. Additionally, since they are almost comparable among the different readers, they also support the good VI-RADS repeatability even in less experienced readers [13]. Interestingly, if, on the one hand, muscle-invasiveness assessment was not significantly different among the three sets of images, the conspicuity varied both qualitatively and quantitatively based on different  $b$ -values. While the best qualitative scores were obtained with set

1, corresponding to the lowest  $b$ -value ( $b = 1000 \text{ s/mm}^2$ ), set 2 led to the best quantitative scores corresponding to intermediate–high  $b$ -value ( $b = 1500 \text{ s/mm}^2$ ). Set 3, which included the highest  $b$ -value ( $b = 2000 \text{ s/mm}^2$ ), showed the lowest qualitative scores and signal intensity at the quantitative analysis. We believe that there are two possible explanations. First, from a quantitative perspective, the reduced signal intensity in the bladder content at higher  $b$ -values

**Table 6** Quantitative assessment of tumor conspicuity for Set 1, Set 2, and Set 3

	Quantitative Assessment									Pairwise Comparison	p-value***		
	Tumor Intensity* (Standard Deviation)			Bladder Content Intensity* (Standard Deviation)			Tumor Conspicuity* (Standard Deviation)					ICC (95% CI**)	
	Set 1	Set 2	Set 3	Set 1	Set 2	Set 3	Set 1	Set 2	Set 3				
<i>Reader 1</i>	1903.36 (741.70)	1907.11 (779.04)	1765.49 (759.19)	562.40 (246.47)	431.09 (122.31)	499.63 (146.01)	4.12 (2.72)	4.74 (2.31)	3.90 (2.29)	0.79 (0.67–0.87)	0.83 (0.74–0.90)	Set 1 vs. Set 2 Set 1 vs. Set 3 Set 3 vs. Set 2	0.012 1.000 0.001
<i>Reader 2</i>	2000.21 (786.60)	1991.77 (789.82)	1799.52 (787.77)	572.58 (200.41)	540.92 (203.88)	517.86 (181.72)	3.92 (2.17)	4.22 (2.41)	3.99 (2.70)				
<i>Reader 3</i>	2083.71 (675.69)	1883.91 (657.04)	1762.44 (697.06)	543.22 (222.29)	434.34 (109.86)	505.44 (159.99)	4.49 (2.30)	4.61 (1.97)	3.83 (1.98)				

\*Mean value

\*\*Confidence Interval

\*\*\*Wilcoxon Test with Bonferroni's correction

resulted in higher tumor conspicuity: the higher background suppression facilitated the tumor visualization. However, the lower intensity in the bladder content corresponded to a reduction of the mean tumor signal intensity compared to lower *b*-values. For this reason, the mean quantitative scores at the highest gradient strengths resulted in low signal intensity of the tumor. In our study, Set 2 resulted in the highest tumor signal intensity, providing the best ratio of background suppression and signal-to-noise reduction. To this end, we recommend using a high-gradient strength DWI using an adequate number of signal average and repetition time to balance the signal-to-noise ratio reduction [18].

Second, to explain the results of qualitative assessment, the use of high *b*-values is burdened with the overall reduced signal, which translates into poor anatomical visualization. The loss of potentially valuable information could thus reduce the diagnostic confidence of the reader. This may be even more evident when an adequate anatomical detail is required, for example, in the bladder wall assessment or in the case of small subtle lesions. In fact, the per-lesion analysis showed the link between the highest gradient strength (*b* = 2000 s/mm<sup>2</sup>) and the increased number of false-negative cases compared to the other sets of images. Most of these cases were due to small (< 5 mm) lesions with substantial overlap among the readers, ranging from 70 to 75%.

To the best of our knowledge, this is the first study comparing the conspicuity and the muscle-invasiveness assessment of different contrast-free bladder MRI settings using VI-RADS in a clinical scenario. By supporting recent studies on the optimization of bladder MRI and the promising results regarding the feasibility of a contrast-free MRI protocol, our results may have a beneficial effect on patient safety costs, scan time, and patient safety [31–33].

Our study has some limitations. First, ours is a single-center study with a relatively low number of patients. Nonetheless, our investigation was intended as a proof-of-concept study. Larger studies, possibly including multiple institutions, are needed to validate our results. Second, the type of VI-RADS scores dichotomization may have represented a selection bias. In fact, the appropriate VI-RADS cut-off defining whether the tumor is muscle invasive is controversial [16, 34]. According to our methodology, Marchioni et al. recently demonstrated that a threshold of 4 significantly improved MIBC detection reaching an accuracy of 90% [16]. Third, the physician experience and the patient characteristics influenced the patient selection. For example, patients with worrisome tumor features (i.e., large and solid tumors) may not have been included to avoid delaying active treatment. Fourth, a degree of unbalanced data (MIBC vs. NMIBC) was present, which could have affected our results. However, considering that our primary aim was to investigate if any difference in terms of conspicuity and muscle-invasiveness assessment among different contrast-free



MRI settings exists, we adopted a multi-reader approach to improve the generalization of our results. Moreover, both per-patient and per-lesion analyses were performed for each reader to test different clinical settings.

## Conclusion

Bladder cancer muscle invasiveness can be accurately assessed using a bi-parametric MRI protocol consisting of T2w and DWI, regardless of the diffusion gradient strengths (1000–2000 s/mm<sup>2</sup>) and the reader's experience. Intermediate-high *b*-value (*b* = 1500 s/mm<sup>2</sup>) showed the highest signal intensity due to an adequate balance between background suppression and signal-to-noise reduction. A *b*-value of 1000 s/mm<sup>2</sup> allowed better tumor–wall interface assessment. Very high *b*-value (*b* = 2000 s/mm<sup>2</sup>) was associated with lower conspicuity and increased false-negative cases, especially for small (< 5 mm) lesions. Further validation studies are warranted to define an optimization of the current bladder MRI protocol and to evaluate the potential clinical role of a contrast-free MRI protocol.

**Acknowledgements** The authors thank Darien Calvo Garcia for his insightful contribution on the MR protocol setting and the acquisition of data.

**Funding** The authors state that this work has not received any funding.

## Declarations

**Conflict of interest** Domenico Mastrodicasa had no activities related to the present article. Activities not related to the present article: shareholder of Segmed, Inc. and consultant for Segmed, Inc. All the other authors of this manuscript declare no relationships with any companies whose products or services may be related to the subject matter of the article. Andrea Delli Pizzi is a member of the Scientific Editorial Board of Insight Into Imaging.

**Ethical approval** All procedures were performed in accordance with the ethical standards of the institutional research committee (Comitato di Etica per la Ricerca Biomedica delle province di Chieti e Pescara e dell'Università degli Studi "G.d'Annunzio" di Chieti e Pescara, no. 1767) and with the 1964 Declaration of Helsinki and its later amendments or comparable ethical standards. Informed consent was obtained from each participant.

**Guarantor** The scientific guarantor of this publication is Andrea Delli Pizzi.

**Informed consent** Written informed consent was obtained from all subjects (patients) in this study.

**Statistics and biometry** No complex statistical methods were necessary for this paper.

**Study subjects or cohorts overlap** The study subjects have been previously reported in the studies: Marchioni, M. et al., Could Bladder Multiparametric MRI Be Introduced in Routine Clinical Practice? Role

of the New VI-RADS Score: Results From a Prospective Study. Clin Genitourin Cancer, 2020. Delli Pizzi, A., Mastrodicasa, D., and Marchioni, M. et al. Bladder cancer: Do we need contrast injection for MRI assessment of muscle invasion? A prospective multi-reader VI-RADS approach. Eur Radiol 31, 3874–3883 (2021). <https://doi.org/10.1007/s00330-020-07473-6>

**Open Access** This article is licensed under a Creative Commons Attribution 4.0 International License, which permits use, sharing, adaptation, distribution and reproduction in any medium or format, as long as you give appropriate credit to the original author(s) and the source, provide a link to the Creative Commons licence, and indicate if changes were made. The images or other third party material in this article are included in the article's Creative Commons licence, unless indicated otherwise in a credit line to the material. If material is not included in the article's Creative Commons licence and your intended use is not permitted by statutory regulation or exceeds the permitted use, you will need to obtain permission directly from the copyright holder. To view a copy of this licence, visit <http://creativecommons.org/licenses/by/4.0/>.

## References

- [1] Bray F, Ferlay J, Soerjomataram I, Siegel RL, Torre LA, Jemal A. Global cancer statistics 2018: GLOBOCAN estimates of incidence and mortality worldwide for 36 cancers in 185 countries. *CA Cancer J Clin*. 2018;68:394-424.
- Richters A, Aben KKH, Kiemeny L. The global burden of urinary bladder cancer: an update. *World J Urol*. 2019.
- [3] Palumbo C, Mistretta FA, Knipper S, Pecoraro A, Tian Z, Shariat SF, et al. How cancer-specific mortality changes over time after radical cystectomy: Conditional survival of patients with nonmetastatic urothelial carcinoma of the urinary bladder. *Urol Oncol*. 2019;37:893-9.
- [4] Zhang N, Wang X, Wang C, Chen S, Wu J, Zhang G, et al. Diagnostic Accuracy of Multi-Parametric Magnetic Resonance Imaging for Tumor Staging of Bladder Cancer: Meta-Analysis. *Front Oncol*. 2019;9:981.
- [5] Panebianco V, Narumi Y, Altun E, Bochner BH, Efsthathiou JA, Hafeez S, et al. Multiparametric Magnetic Resonance Imaging for Bladder Cancer: Development of VI-RADS (Vesical Imaging-Reporting And Data System). *Eur Urol*. 2018;74:294-306.
- Woo S, Panebianco V, Narumi Y, Del Giudice F, Muglia VF, Takeuchi M, et al. Diagnostic Performance of Vesical Imaging Reporting and Data System for the Prediction of Muscle-invasive Bladder Cancer: A Systematic Review and Meta-analysis. *Eur Urol Oncol*. 2020.
- [7] Babjuk M, Bohle A, Burger M, Capoun O, Cohen D, Comperat EM, et al. EAU Guidelines on Non-Muscle-invasive Urothelial Carcinoma of the Bladder: Update 2016. *Eur Urol*. 2017;71:447-61.
- [8] Hurler R, Lazzeri M, Vanni E, Lughezzani G, Buffi N, Casale P, et al. Active Surveillance for Low Risk Nonmuscle Invasive Bladder Cancer: A Confirmatory and Resource Consumption Study from the BIAS Project. *J Urol*. 2018;199:401-6.
- [9] Schips L, Augustin H, Zigeuner RE, Galle G, Habermann H, Trummer H, et al. Is repeated transurethral resection justified in patients with newly diagnosed superficial bladder cancer? *Urology*. 2002;59:220-3.
- [10] McKibben MJ, Woods ME. Preoperative imaging for staging bladder cancer. *Curr Urol Rep*. 2015;16:22.
- [11] Watanabe H, Kanematsu M, Kondo H, Goshima S, Tsuge Y, Onozuka M, et al. Preoperative T staging of urinary bladder

- cancer: does diffusion-weighted MRI have supplementary value? *AJR Am J Roentgenol.* 2009;192:1361-6.
12. [12] Del Giudice F, Barchetti G, De Berardinis E, Pecoraro M, Salvo V, Simone G, et al. Prospective Assessment of Vesical Imaging Reporting and Data System (VI-RADS) and Its Clinical Impact on the Management of High-risk Non-muscle-invasive Bladder Cancer Patients Candidate for Repeated Transurethral Resection. *Eur Urol.* 2020;77:101-9.
  13. [13] Barchetti G, Simone G, Ceravolo I, Salvo V, Campa R, Del Giudice F, et al. Multiparametric MRI of the bladder: inter-observer agreement and accuracy with the Vesical Imaging-Reporting and Data System (VI-RADS) at a single reference center. *Eur Radiol.* 2019;29:5498-506.
  14. [14] Thoeny HC, Bellin MF, Comperat EM, Thalmann GN. Vesical Imaging-Reporting and Data System (VI-RADS): Added Value for Management of Bladder Cancer Patients? *Eur Urol.* 2018;74:307-8.
  15. [15] Makkoul M, Farghaly S, Abdelkawi IF. Multiparametric MRI in differentiation between muscle invasive and non-muscle invasive urinary bladder cancer with vesical imaging reporting and data system (VI-RADS) application. *Br J Radiol.* 2019;92:20190401.
  16. Marchioni M, Primiceri G, Delli Pizzi A, Basilico R, Berardinelli F, Mincuzzi E, et al. Could Bladder Multiparametric MRI Be Introduced in Routine Clinical Practice? Role of the New VI-RADS Score: Results From a Prospective Study. *Clin Genitourin Cancer.* 2020.
  17. Delli Pizzi A, Mastrodicasa D, Marchioni M, Primiceri G, Di Fabio F, Cianci R, et al. Bladder cancer: do we need contrast injection for MRI assessment of muscle invasion? A prospective multi-reader VI-RADS approach. *European Radiology.* 2020.
  18. [18] Delli Pizzi A, Caposiena D, Mastrodicasa D, Trebeschi S, Lambregts D, Rosa C, et al. Tumor detectability and conspicuity comparison of standard b1000 and ultrahigh b2000 diffusion-weighted imaging in rectal cancer. *Abdom Radiol (NY).* 2019;44:3595-605.
  19. [19] Fukukura Y, Kumagai Y, Hakamada H, Shindo T, Takumi K, Kamimura K, et al. Computed diffusion-weighted MR imaging for visualization of pancreatic adenocarcinoma: Comparison with acquired diffusion-weighted imaging. *European Journal of Radiology.* 2017;95:39-45.
  20. Gakis G, Tamada T, Kanomata N, Sone T, Jo Y, Miyaji Y, et al. High  $b$  Value ( $2,000 \text{ s/mm}^2$ ) Diffusion-Weighted Magnetic Resonance Imaging in Prostate Cancer at 3 Tesla: Comparison with  $1,000 \text{ s/mm}^2$  for Tumor Conspicuity and Discrimination of Aggressiveness. *PLoS ONE.* 2014;9.
  21. [21] Hausmann D, Liu J, Budjan J, Reichert M, Ong M, Meyer M, et al. Image Quality Assessment of 2D versus 3D T2WI and Evaluation of Ultra-high  $b$ -Value ( $b=2,000 \text{ mm}^2/\text{s}$ ) DWI for Response Assessment in Rectal Cancer. *Anticancer Res.* 2018;38:969-78.
  22. [22] Moribata Y, Kido A, Fujimoto K, Himoto Y, Kurata Y, Shitano F, et al. Feasibility of Computed Diffusion Weighted Imaging and Optimization of  $b$ -value in Cervical Cancer. *Magn Reson Med Sci.* 2017;16:66-72.
  23. [23] Ueno Y, Kitajima K, Sugimura K, Kawakami F, Miyake H, Obara M, et al. Ultra-high  $b$ -value diffusion-weighted MRI for the detection of prostate cancer with 3-T MRI. *J Magn Reson Imaging.* 2013;38:154-60.
  24. [24] Haak HE, Maas M, Lahaye MJ, Boellaard TN, Delli Pizzi A, Muhl C, et al. Selection of Patients for Organ Preservation After Chemoradiotherapy: MRI Identifies Poor Responders Who Can Go Straight to Surgery. *Ann Surg Oncol.* 2020;27:2732-9.
  25. [25] Rosa C, Caravatta L, Delli Pizzi A, Di Tommaso M, Cianci R, Gasparini L, et al. Reproducibility of rectal tumor volume delineation using diffusion-weighted MRI: Agreement on volumes between observers. *Cancer Radiother.* 2019;23:216-21.
  26. [26] Rosenkrantz AB, Hindman N, Lim RP, Das K, Babb JS, Mussi TC, et al. Diffusion-weighted imaging of the prostate: Comparison of b1000 and b2000 image sets for index lesion detection. *J Magn Reson Imaging.* 2013;38:694-700.
  27. [27] Necchi A, Bandini M, Calareso G, Raggi D, Pederzoli F, Fare E, et al. Multiparametric Magnetic Resonance Imaging as a Noninvasive Assessment of Tumor Response to Neoadjuvant Pembrolizumab in Muscle-invasive Bladder Cancer: Preliminary Findings from the PURE-01 Study. *Eur Urol.* 2020;77:636-43.
  28. Necchi A, Messina A, Briganti A. Re: Valeria Panebianco, Yoshifumi Narumi, Ersan Altun, et al. Multiparametric Magnetic Resonance Imaging for Bladder Cancer: Development of VI-RADS (Vesical Imaging-Reporting And Data System). *Eur Urol* 2018;74:294–306: Validating VI-RADS Criteria Within Immunonecology Strategies (VI-RADS-IO). *Eur Urol.* 2018;74:e107-e8.
  29. Del Giudice F, Catto JWF, Panebianco V. Reply to Charalampos Fragkoulis, Georgios Papadopoulos, and Konstantinos Ntoumas's Letter to the Editor re: Francesco Del Giudice, Giovanni Barchetti, Ettore De Berardinis, et al. Prospective Assessment of Vesical Imaging Reporting and Data System (VI-RADS) and its Clinical Impact on the Management of High-risk Non-muscle-invasive Bladder Cancer Patients Candidate for Repeated Transurethral Resection. *Eur Urol* 2020;77:101–9. *Eur Urol.* 2020;77:e94-e5.
  30. [30] Juri H, Narumi Y, Panebianco V, Osuga K. Staging of bladder cancer with multiparametric MRI. *Br J Radiol.* 2020;93:20200116.
  31. Gmeiner J, Garstka N, Helbich TH, Shariat SF, Baltzer PA. Vesical Imaging Reporting and Data System (VI-RADS): Are the individual MRI sequences equivalent in diagnostic performance of high grade NMIBC and MIBC? *Eur J Radiol.* 2021;142:109829.
  32. Rabie E, Faeghi F, Izadpanahi MH, Dayani MA. Role of Dynamic Contrast-Enhanced Magnetic Resonance Imaging in Staging of Bladder Cancer. *J Clin Diagn Res.* 2016;10:TC01–5.
  33. [33] Takeuchi M, Suzuki T, Sasaki S, Ito M, Hamamoto S, Kawai N, et al. Clinicopathologic significance of high signal intensity on diffusion-weighted MR imaging in the ureter, urethra, prostate and bone of patients with bladder cancer. *Acad Radiol.* 2012;19:827-33.
  34. [34] Wang H, Luo C, Zhang F, Guan J, Li S, Yao H, et al. Multiparametric MRI for Bladder Cancer: Validation of VI-RADS for the Detection of Detrusor Muscle Invasion. *Radiology.* 2019;291:668-74.

**Publisher's Note** Springer Nature remains neutral with regard to jurisdictional claims in published maps and institutional affiliations.

## Authors and Affiliations

Andrea Delli Pizzi<sup>1</sup>  · Domenico Mastrodicasa<sup>2</sup> · Alessio Taraschi<sup>3</sup> · Nicoletta Civitareale<sup>3</sup> · Erica Mincuzzi<sup>3</sup> · Stefano Censi<sup>4</sup> · Michele Marchioni<sup>5,6</sup> · Giulia Primiceri<sup>5</sup> · Pietro Castellan<sup>5</sup> · Roberto Castellucci<sup>5</sup> · Giulio Cocco<sup>7</sup> · Piero Chiacchiaretta<sup>8,9</sup> · Antonella Colasante<sup>10</sup> · Antonio Corvino<sup>11</sup> · Luigi Schips<sup>5</sup> · Massimo Caulo<sup>4</sup>

Domenico Mastrodicasa  
domenico.mastrodicasa@gmail.com

Alessio Taraschi  
alessiolinotaraschi@gmail.com

Nicoletta Civitareale  
nic.civitareale@gmail.com

Erica Mincuzzi  
erica.mincuzzi@gmail.com

Stefano Censi  
stefano.censi@studenti.unich.it

Michele Marchioni  
mic.marchioni@gmail.com

Giulia Primiceri  
giulia.primiceri@gmail.com

Pietro Castellan  
castellanpietro@gmail.com

Roberto Castellucci  
roberto.castellucci@gmail.com

Giulio Cocco  
cocco.giulio@gmail.com

Piero Chiacchiaretta  
piero.chiacchiaretta@gmail.com

Antonella Colasante  
acolasante61@gmail.com

Antonio Corvino  
an.cor@hotmail.it

Luigi Schips  
luigischips@hotmail.com

Massimo Caulo  
massimo.caulo@gmail.com

<sup>1</sup> Department of Innovative Technologies in Medicine & Dentistry, “G. d’Annunzio” University, Chieti, Italy

<sup>2</sup> Department of Radiology, Stanford University School of Medicine, Stanford, CA, USA

<sup>3</sup> Unit of Radiology, “Santissima Annunziata” Hospital, Chieti, Italy

<sup>4</sup> Department of Neuroscience, Imaging and Clinical Sciences, “G. d’Annunzio” University, Chieti, Italy

<sup>5</sup> Department of Medical, Oral and Biotechnological Sciences, G. d’Annunzio University of Chieti, Urology Unit, SS Annunziata Hospital, Chieti, Italy

<sup>6</sup> Laboratory of Biostatistics, Department of Medical, Oral and Biotechnological Sciences, “G. D’Annunzio” University, Chieti, Italy

<sup>7</sup> Unit of Ultrasound in Internal Medicine, Department of Medicine and Science of Aging, “G. D’Annunzio” University, Chieti, Italy

<sup>8</sup> Center of Advanced Studies and Technology (CAST), “G. d’Annunzio” University of Chieti-Pescara, Chieti, Italy

<sup>9</sup> Department of Psychological, Health and Territory Sciences, “G. d’Annunzio” University of Chieti-Pescara, Chieti, Italy

<sup>10</sup> Surgical Pathology Unit, SS Annunziata Hospital, Chieti, Italy

<sup>11</sup> Motor Science and Wellness Department, University of Naples “Parthenope”, Naples, Italy